

The Top Quark Decay Vertex in Standard Model Extensions

Werner Bernreuther^{*}, Patrick González[†], Martin Wiebusch[‡]

Institut für Theoretische Physik, RWTH Aachen University, 52056 Aachen, Germany

Abstract

New physics interactions can affect the strength and structure of the tbW vertex. We investigate the magnitudes and phases of “anomalous” contributions to this vertex in a two-Higgs doublet and the minimal supersymmetric extension of the standard model, and in a top-color assisted technicolor (TC2) model. While the magnitudes of the anomalous couplings remain below 1 percent in the first two models, TC2 interactions can reduce the left-chiral coupling f_L by several percent.

PACS number(s): 11.30.Er, 12.60.-i, 14.65.Ha

Keywords: top quark decay, anomalous form factors, standard model extensions

^{*}Email: breuther@physik.rwth-aachen.de

[†]Email: gonzalez@physik.rwth-aachen.de

[‡]Email: mwiebusch@physik.rwth-aachen.de

1. Introduction

The decays of top quarks are a direct and sensitive probe of the fundamental interactions at energy scales of a few hundred GeV. So far all data from the Tevatron are compatible with the predictions from the Standard Model (SM). Only the decay mode $t \rightarrow Wb$ has been detected [1], which is predicted by the SM to completely dominate the top-decay rate. SM extensions (BSM) suggest that exotic decay modes of the top quark may exist, with branching ratios being observable at the Tevatron or eventually at the Large Hadron Collider (LHC). Well-known examples include the decay into a relatively light charged Higgs boson, $t \rightarrow bH^+$, or into a light top-squark and the lightest neutralino, $t \rightarrow \tilde{t}_1 \tilde{\chi}_1$, which is possible in the (minimal) supersymmetric SM extension (MSSM). (See, for instance, the reviews [2–5]). BSM physics affecting top quarks need not lead to new decay modes, because of kinematic obstructions. In any case, it should leave its mark on the strength and structure of the tbW vertex. Parameterizing BSM contributions to the vertex by “anomalous” couplings, one can obtain direct information on these couplings from the fractions $F_{0,\mp}$ of $t \rightarrow bW^+$ decays with W -boson helicity $\lambda_W = 0, \mp 1$, and from single top-quark production. While the sensitivity to BSM effects on $F_{0,\mp}^{exp}$ [6–9] and on single-top-quark production [10–13] from the Tevatron is rather modest, one expects that these anomalous form factors can be determined quite precisely at the LHC [14–18].

On the theoretical side, there have been a number of investigations on new physics contributions to $t \rightarrow Wb$ decay, including two-Higgs doublet models (2HDM) [19, 20], the minimal supersymmetric extension of the standard model (MSSM) [21–26], top-color assisted technicolor models (TC2) [27], and Little Higgs models [28–30]. In these papers, the corrections to the decay rate and, in some cases, also to the helicity fractions were analyzed.

In this paper we investigate the tbW vertex in a number of SM extensions, i.e., we compute the induced anomalous charged current couplings, revisiting and extending previous results in the literature. Our primary concern is to investigate whether BSM models predict large enough values for these couplings to be detectable at the LHC. In Section 2 we specify our convention for these form factors and recapitulate their CP transformation properties. We briefly review what is presently known from experiments about these couplings, and recall the sensitivities with which they are expected to be measurable at the LHC. In Section 3 we compute these anomalous couplings at the 1-loop level in the type-II two-Higgs doublet model, in the MSSM, and in a TC2 model. For completeness we recapitulate also some results from Little Higgs models. Apart from determining the magnitude of these form factors, we investigate also their phases. In the context of these models this provides a check of the assumption, often made in simulation studies [14, 15, 17], that these couplings are real to a good approximation. We conclude in Section 4.

2. The tbW vertex: status and expectations

As is well-known, a model-independent analysis of the structure of the tbW vertex can be made using a form-factor decomposition. The amplitude \mathcal{M}_{tbW} of the decay $t(p) \rightarrow b(k)W^+(q)$, where all particles are on-shell, can be decomposed in terms of four form factors:

$$\mathcal{M}_{tbW^+} = -\frac{g_W}{\sqrt{2}}\epsilon^{\mu*} \bar{u}_b \left[(V_{tb}^* + f_L)\gamma_\mu P_L + f_R\gamma_\mu P_R + i\sigma_{\mu\nu}q^\nu \left(\frac{g_L}{m_W}P_L + \frac{g_R}{m_W}P_R \right) \right] u_t, \quad (2.1)$$

with $P_{L,R} = (1 \mp \gamma_5)/2$. Here V_{tb} is the Cabibbo-Kobayashi-Maskawa (CKM) matrix element in the three-generation SM, and p , k , and $q = p - k$ denote the four-momenta of the t and b quark and the W boson, respectively. The two chirality conserving and flipping form factors $f_{L,R}$ and $g_{L,R}$, respectively, are dimensionless (complex) functions of q^2 . If the W boson is off-shell, two additional form factors appear in the matrix element (2.1). However, they do not contribute to the matrix element of $t \rightarrow b f_1 \bar{f}_2$ in the limit of vanishing fermion masses $m_{f_{1,2}}$.

The parameterization in (2.1) is chosen in such a way that non-zero values of $f_{L,R}$ and $g_{L,R}$ signify deviations from the structure of the tree-level Born vertex. They are generated by SM loop corrections and, possibly, by new physics interactions. In the SM and in SM extensions which correspond to renormalizable theories, $f_{L,R} \neq 0$ can appear at tree-level while $g_{L,R} \neq 0$ must be loop-induced. Notice that a significant deviation of $|V_{tb}|_{exp}$ from ~ 0.99 is a possibility which is not yet experimentally excluded [31]. In our parameterization (2.1) this would imply a sizeable coupling $f_L \neq 0$.

The form factors are gauge-invariant but are not, in general, infrared-finite. They should be used to parameterize only new ‘‘infrared safe’’ short-distance contributions to the tbW vertex, caused for instance by the exchange of new heavy virtual particles. A search for anomalous couplings in $t \rightarrow bW$ decay-data should use the following matrix elements: a) The SM decay distributions $d\Gamma_{SM}$ including radiative corrections, which are presently known to NLO in the gauge couplings, that is, for $t \rightarrow Wb$, $t \rightarrow Wb\gamma$, and $t \rightarrow bWg$. b) One adds to $d\Gamma_{SM}$ the contributions $d\Gamma_{BSM}$ linear in the ‘‘anomalous’’ form factors $f_{L,R}$ and $g_{L,R}$, which are generated by the interference of (2.1) with the SM Born amplitude, and possibly also the terms bilinear¹ in $f_{L,R}$, $g_{L,R}$. In the following we use the convention that $f_{L,R}$ and $g_{L,R}$ parameterize only the new physics contributions to $t \rightarrow bW$.

The amplitude of the charge-conjugate decay $\bar{t}(\bar{p}) \rightarrow \bar{b}(\bar{k})W^-(\bar{q})$ has the general structure:

$$\mathcal{M}_{\bar{t}\bar{b}W^-} = -\frac{g_W}{\sqrt{2}}\epsilon^{\mu*} \bar{v}_t \left[(V_{tb} + f'_L)\gamma_\mu P_L + f'_R\gamma_\mu P_R + i\sigma_{\mu\nu}\bar{q}^\nu \left(\frac{g'_R}{m_W}P_L + \frac{g'_L}{m_W}P_R \right) \right] v_b. \quad (2.2)$$

¹Within a specific SM extension, these linear and bilinear terms must, of course, be incorporated consistently in a perturbative calculation.

	f_L	f_R	g_L	g_R
upper bound	0.03	0.0025	0.0004	0.57
lower bound	-0.13	-0.0007	-0.0015	-0.15

Table 1: Current 95 % C.L. upper and lower bounds on the anomalous form factors in the tbW vertex from $B(\bar{B} \rightarrow X_s \gamma)$ [37]. Here the form factors were assumed to be real.

CP invariance requires, apart from V_{tb} being real, that the form factors in (2.1), (2.2) satisfy² [32]:

$$f'_i = f_i, \quad g'_i = g_i \quad (i = R, L). \quad (2.3)$$

CPT invariance implies another useful set of relations. If absorptive parts of the form factors are neglected, then

$$f'_i = f_i^*, \quad g'_i = g_i^* \quad (i = R, L). \quad (2.4)$$

These relations imply the following: If absorptive parts (i.e., final-state interactions) can be neglected, then CPT invariance enforces the real parts of the form factors to be equal, even if CP is violated:

$$\text{Re } f'_i = \text{Re } f_i, \quad \text{Re } g'_i = \text{Re } g_i \quad (i = R, L). \quad (2.5)$$

In this case CP violation induces non-zero imaginary parts which are equal in magnitude but differ in sign, namely,

$$\text{Im } f'_i = -\text{Im } f_i, \quad \text{Im } g'_i = -\text{Im } g_i \quad (i = R, L). \quad (2.6)$$

Non-zero absorptive parts of the decay amplitude also lead to imaginary parts of the form factors. If CP is conserved they are equal in magnitude and sign. If CP is broken then CP -violating absorptive parts of the decay amplitude can contribute to the real parts of the form factors and violate (2.5). Suffice it to say that CP violation at an observable level in the CKM-allowed decay $t \rightarrow bW \rightarrow bq\bar{q}'$ would be a clear sign of a non-SM CP -violating interaction. CKM induced CP violation in these decay modes is unobservably small, as it is a higher loop effect proportional to $J_{CP} = \text{Im}(V_{tb}V_{cd}V_{td}^*V_{cb}^*) \simeq 3 \times 10^{-5}$.

For a small $V+A$ admixture to the SM current, energy and higher-dimensional distributions were computed in the fashion described above eq. (2.2) in [33, 34]. In this case neutrino energy-angular distributions turn out to be most sensitive to $f_R \neq 0$. It is important to take the QCD corrections into account in (future) data analyses, as gluon radiation can mimic a small $V+A$ admixture.

There are indirect constraints on some of the anomalous couplings from the measured branching ratio $B(\bar{B} \rightarrow X_s \gamma)$. In particular the constraints on f_R and g_L – that is, the couplings to

²In [32] a different convention was used for the amplitude (2.2).

a right-chiral b quark – are tight, as the contributions of these couplings to the respective B -meson decay amplitude are enhanced by a factor m_t/m_b [35, 36]. A recent analysis [37] arrives at the bounds given in table 1. (For earlier work, see [38, 39].) These bounds were obtained by allowing only one coupling to be non-zero at a time. Obviously, these bounds are no substitute for direct measurements, as the contributions of different couplings to this decay rate might cancel among each other or might be off-set by other new physics contributions.

A basic direct test of the structure of the tbW vertex is the measurement of the decay fractions $F_0 = B(t \rightarrow bW(\lambda_W = 0))$, $F_{\mp} = B(t \rightarrow bW(\lambda_W = \mp 1))$ into W^+ bosons of helicity $\lambda_W = 0, \mp 1$. (By definition $F_0 + F_- + F_+ = 1$.) Their SM values are known, including the $O(\alpha_s)$ QCD and $O(\alpha)$ electroweak corrections [40], which are, in fact, small corrections. For $m_t = 172$ GeV, $F_0 = 0.689$, $F_- = 0.310$, $F_+ = 0.001$ in the SM. The dependence on the anomalous couplings (2.1) of the helicity fractions $F_{0,\pm}$ can be obtained in straightforward fashion. Corresponding expressions can be found, for instance, in [16, 41]. The fractions $F_{0,\pm}$ are sensitive only to ratios of couplings. The top width Γ_t is an observable which is sensitive also to the absolute strength of the tbW vertex. However, no method is presently known to measure Γ_t with reasonable precision at a hadron collider. Single top-quark production is the means to get a handle on the strength of the tbW vertex, and in particular on f_L . In the SM, top quarks can be produced singly at hadron colliders by t -channel reactions ($qb \rightarrow q't$), which are the dominant production processes both at the Tevatron and at the LHC, by s -channel reactions ($q\bar{q}' \rightarrow t\bar{b}$), and by associated production $gb \rightarrow tW^-$. Assuming that new physics effects in these processes reside in the tbW vertex only, one can compute the corresponding cross sections in terms of the above anomalous couplings [18, 41–44]. The single top processes may eventually be separately measurable at the LHC. The four anomalous couplings (2.1) may, in principle, be determined simultaneously from the observables $F_{0,\pm}$ and the separately measured single-top cross sections, if these quantities will be measured with sufficient precision. This should eventually be feasible at the LHC. In addition to the helicity fractions, energy and energy-angular distributions in polarized semi- and non-leptonic top-quark decays turn out to be good probes for f_R [33, 34] and g_R [15]. (Cf. also [45–47].)

The CDF and D0 experiments at the Tevatron have measured the helicity fractions from top quark decays in $t\bar{t}$ events [6–9]. Furthermore, both the D0 and the CDF experiment have found evidence for single top quark production [10, 11, 13], and the D0 collaboration has recently made a search for anomalous couplings [12] based on their measurement of σ_t . Both the measured helicity fractions and the D0 and CDF results for σ_t are compatible with SM expectations. The level of precision with which these observables are presently known does not imply constraints on $f_{L,R}$ and $g_{L,R}$ that can compete with the indirect bounds of table 1.

However, future high statistics data on top quark decays at the LHC will allow direct determination of the couplings f_R, g_L , and g_R with an accuracy of a few percent³. Simulation studies analyzed $t\bar{t}$ production and decay into lepton plus jets channels [14, 15, 17] and also dileptonic channels [14]. Basic observables for determining the anomalous couplings are the W -boson helicity fractions and associated forward-backward asymmetries [17]. A double angular distribution in t -quark decay was used in [15]. These simulation studies assumed f_L to be zero and the other form factors to be real. The parametric dependence of the observables on the anomalous couplings yields estimates for the expected confidence intervals. Assuming that only one non-standard coupling is nonzero at a time, [17] concludes that values of f_R, g_L , or g_R outside the following intervals,

$$f_R(2\sigma) : [-0.055, 0.13], \quad g_L(2\sigma) : [-0.058, 0.026], \quad g_R(2\sigma) : [-0.026, 0.031], \quad (2.7)$$

should be either detected or excluded at the 2 s.d. level (statistical and systematic uncertainties). The analyses of [14] and of [15] arrived, as far as g_R is concerned, at a sensitivity level of the same order. Thus the sensitivity to g_R expected at the LHC is an order of magnitude better than the current indirect bound given in table 1.

An analysis was recently made [18] combining single top-quark production and top-quark decay (from $t\bar{t}$ events) and expected experimental uncertainties at the LHC. (For related work, see [41, 42, 44].) Assuming all form factors to be real, this analysis concludes that a simultaneous four-parameter fit to respective data yields the 1σ sensitivities

$$\begin{aligned} f_L(1\sigma) &: [-0.15, 0.11], & f_R(1\sigma) &: [-0.25, 0.25], \\ g_L(1\sigma) &: [-0.16, 0.16], & g_R(1\sigma) &: [-0.012, 0.024]. \end{aligned} \quad (2.8)$$

The sensitivity to g_R is essentially as good as the one obtained in the one-parameter analysis (2.7).

As discussed above, the form factors $f_{L,R}$ and $g_{L,R}$ can be complex, due to final-state interactions or CP violation. CP -violating contributions to the absorptive parts of the form factors are real and invalidate the relations (2.5). Well-known observables which require non-zero CP -violating absorptive parts are asymmetries of partial decay rates. For instance⁴:

$$A_{CP} = \frac{\Gamma(t \rightarrow bW^+) - \Gamma(\bar{t} \rightarrow \bar{b}W^-)}{\Gamma(t \rightarrow bW^+) + \Gamma(\bar{t} \rightarrow \bar{b}W^-)}. \quad (2.9)$$

An observable which does not require CP -violating absorptive parts to be non-zero is the expectation value of the T -odd triple correlation $O = \mathbf{S}_t \cdot (\hat{\mathbf{p}}_{\ell^+} \times \hat{\mathbf{p}}_b)$ in polarized semileptonic t decay, $t \rightarrow b\ell^+\nu_\ell$. Here \mathbf{S}_t denotes the top spin and the hat signifies a unit vector. This

³Effects of anomalous couplings in the CKM-suppressed tsW vertex were studied in [48].

⁴The asymmetry A_{CP} is CP -odd and CPT -odd, where T refers to a naive T transformation.

correlation is sensitive both to CP -invariant absorptive parts and to CP violation in the tbW vertex. By measuring O and the corresponding correlation \bar{O} in t and \bar{t} decay, respectively, one can disentangle CP -violating effects from CP -invariant absorptive parts. Taking the difference constitutes a CP -symmetry test in top-quark decay, while the sum picks up the CP -invariant imaginary parts⁵. One finds that $\langle O \rangle \mp \langle \bar{O} \rangle \propto \text{Im}(g_R \mp g'_R)$ [32, 51].

At the LHC only single-top-production can provide highly polarized samples of t and \bar{t} quarks. They are mostly produced by the t -channel reactions $qb \rightarrow q't$ (and likewise, \bar{t}). It is known [52] that the sample of t quarks produced by these processes is almost 100% polarized in the direction of the spectator jet q' , with the jet direction determined in the top-quark rest frame. The sample of \bar{t} quarks, produced by the corresponding t -channel processes, has a polarization degree of -100% with respect to the direction of the spectator jet. Alternatively, one can also use the direction of one of the proton beams as the t and \bar{t} spin axis [52]. These results were obtained assuming SM interactions in the production process. If new physics effects result only in modifications of the tbW vertex according to (2.1), it can be shown that the spectator jet directions remain optimal t and \bar{t} spin axes, as long as $|f_R|, |g_{L,R}| \ll 1$.

If LHC experiments will eventually be able to collect clean samples of single t and \bar{t} events (with charge tagging through their semileptonic decays), then one may measure

$$A_{\mp} = \langle \hat{\mathbf{p}} \cdot (\hat{\mathbf{p}}_{\ell^+} \times \hat{\mathbf{p}}_b) \rangle_t \mp \langle \hat{\mathbf{p}} \cdot (\hat{\mathbf{p}}_{\ell^-} \times \hat{\mathbf{p}}_{\bar{b}}) \rangle_{\bar{t}}, \quad (2.10)$$

where $\hat{\mathbf{p}}$ is the direction of one of the proton beams in the t (\bar{t}) rest frame. Again, A_- is sensitive to possible CP -violating effects, in particular to CP -violating effects in top-quark decay, while A_+ is fed by CP -invariant absorptive parts. (One should keep in mind, however, that A_- is not CP -odd in the strict sense, as the initial pp state is not a CP eigenstate.) The number of single t and \bar{t} quarks that will be produced at the LHC is huge. Thus a statistical error $\delta A_{\mp}^{stat} \sim 1\%$ in the measurement of A_{\mp} seems realistic. However, it remains to be investigated whether the systematic uncertainties can reach the same level of precision.

3. Form factors in SM extensions

In this section we compute, within the framework of several SM extensions, the new physics contributions to the form factors $f_{L,R}$ and $g_{L,R}$. To begin with, we briefly recapitulate the SM results for the top-quark decay width Γ_t and differential distributions. The first-order QCD and electroweak corrections to Γ_t were first computed in [53] and [54, 55], respectively. The

⁵Other CP asymmetries in top-quark decay were discussed in [49]. QCD-induced T-odd asymmetries in $t \rightarrow b\ell\nu_{\ell}g$ were investigated in [50].

$O(\alpha_s^2)$ corrections to Γ_t are also known [56, 57]. Essentially, only the QCD corrections matter and these amount to corrections of about minus 10% with respect to the Born width. The first-order SM corrections to the helicity fractions $F_{0,\pm}$, which are small, were determined in [40]. Various distributions for (polarized) semileptonic and non-leptonic top-quark decay were calculated to $O(\alpha_s)$ by [58–60] and [60, 61], respectively. As to the structure of the 1-loop decay amplitude \mathcal{M}_{tbW} in the SM: for $m_b \rightarrow 0$ the form factors f_R^{SM} and g_L^{SM} vanish, as these couplings accompany Lorentz structures that involve a right-chiral b quark. Virtual photon and gluon exchange lead to infrared-divergent 1-loop SM form factors. These infrared divergences in $d\Gamma$ are cancelled, as usual, by the contributions from real soft photon and gluon radiation.

Throughout this paper we shall use the following SM parameters:

$$\begin{aligned} 1/\alpha_{\text{em}} = 137.035999679, \quad \alpha_s = 0.1176, \quad m_Z = 91.1876 \text{ GeV}, \quad m_W = 80.398 \text{ GeV}, \\ m_t = 172.6 \text{ GeV}, \quad m_b = 4.79 \text{ GeV}, \quad V_{tb} = 1. \end{aligned} \quad (3.1)$$

Furthermore, all new physics contributions are calculated relative to the SM corrections with a Higgs-boson mass of 120 GeV.

3.1. Two-Higgs doublet extensions

Two-Higgs doublet models (2HDM) are among the simplest, phenomenologically viable SM extensions. They are often used as a paradigm for an extended Higgs-boson sector, which entails new physics effects, for instance Higgs sector CP violation. Within the supersymmetric framework, two Higgs doublet fields are the minimum requirement for the Higgs sector of a supersymmetric extension of the SM.

Here we consider a general type-II 2HDM, where the Higgs doublets ϕ_1 and ϕ_2 couple only to right-handed down-type fermions (d_{iR}, ℓ_{iR}) and up-type fermions (u_{iR}, v_{iR}), respectively. First we assume the tree-level Higgs potential to be CP -invariant. The spin-0 physical particle spectrum of this model consists of two neutral scalar and one pseudoscalar Higgs boson, h^0, H^0 and A^0 , respectively, and a charged Higgs boson and its antiparticle, H^\pm . Besides the Higgs boson masses $m_{h^0}, m_{H^0}, m_{A^0}$, and m_{H^\pm} the model involves two more free parameters, which are commonly defined as angles, namely, $\tan\beta = v_2/v_1$, where $v_{1,2}$ are the vacuum expectation values of the Higgs fields $\phi_{1,2}$. The angle α describes the mixing of the two CP -even neutral Higgs states which leads to the mass eigenstates h^0 and H^0 .

Experiments that searched for neutral and charged Higgs bosons exclude, when analyzed in the framework of type-II 2HDM, various regions in the parameter space of the model; see, for instance, [62]. The masses of the neutral Higgs states are, in general, constrained to be not smaller than about 100 GeV [63]. The non-observation of $e^+e^- \rightarrow H^+H^-$ at LEP2

provides the model-independent lower bound $m_{H^+} > 79.3$ GeV [63]. However, the rare decay mode $B(\bar{B} \rightarrow X_s \gamma)$ implies, when analyzed within the type-II 2HDM, the much more stringent bound $m_{H^+} > 315$ GeV [64], which holds for all values of $\tan\beta$. The 1-loop Higgs

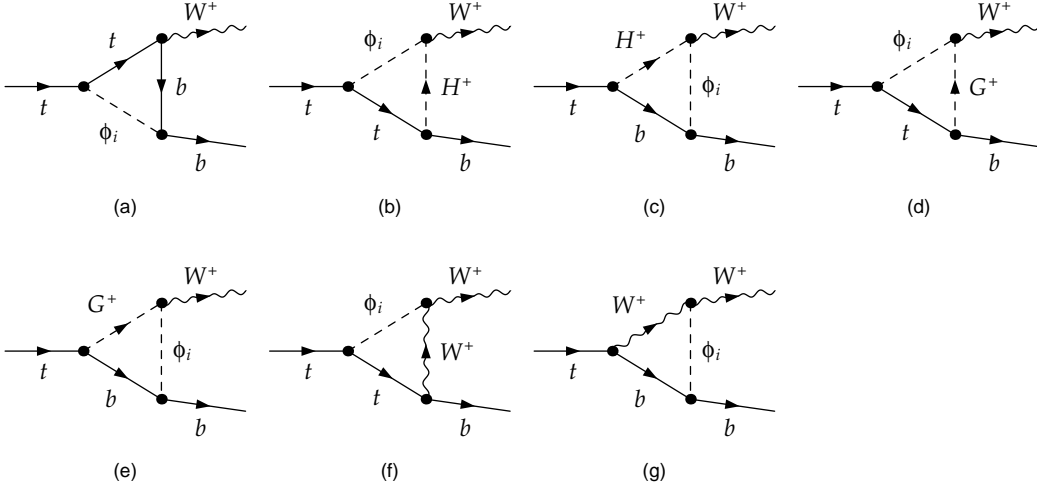


Figure 1: Feynman diagrams for the Higgs boson contributions to the tbW vertex in the type-II 2HDM. In the case of a 2HDM with CP -conserving Higgs potential, the symbol ϕ_i denotes the neutral bosons h^0, H^0 and A^0 . In this case, only the CP -even states $\phi_i = h^0, H^0$ contribute in Figs. (d), (e), (f), and (g). The self-energy corrections that are involved in the renormalization are not shown.

boson contributions to the $t \rightarrow bW$ amplitude in the type-II 2HDM are shown in Fig. 1. The resulting contributions to the decay width $\Gamma(t \rightarrow bW)$ were computed in [19, 20]. Besides using the on-shell renormalization scheme a suitable choice is to parameterize the lowest order width in terms of the Fermi constant G_F rather than in terms of the fine structure constant α , in order to avoid large SM corrections [54]. The relation between the Born widths in both schemes is $\Gamma_B(G_F) = \Gamma_B(\alpha)/(1 - \Delta r)$, where the well-known quantity Δr summarizes the radiative corrections to muon decay [19, 20]. We also adopt this scheme here and in the computations within the other models below. We have compared our results of the non-standard corrections $\delta_{NS}(G_F) = (\Gamma_{NS} - \Gamma_B(G_F))/\Gamma_B(G_F)$ to the Born width with those of [19, 20] and find agreement. Here and below, we have used the *FeynArts* [65, 66], *FormCalc* [67–70], and *LoopTools* [67] packages to perform our calculations.

For this comparison and for the following calculations we have subtracted the contribution of a Higgs boson with SM couplings from the contributions of the diagrams of Fig. 1, in order to define the non-standard corrections. The mass of the SM Higgs boson is chosen to be 120 GeV. The Higgs boson masses and $\tan\beta$ of the 2HDM are varied in the following

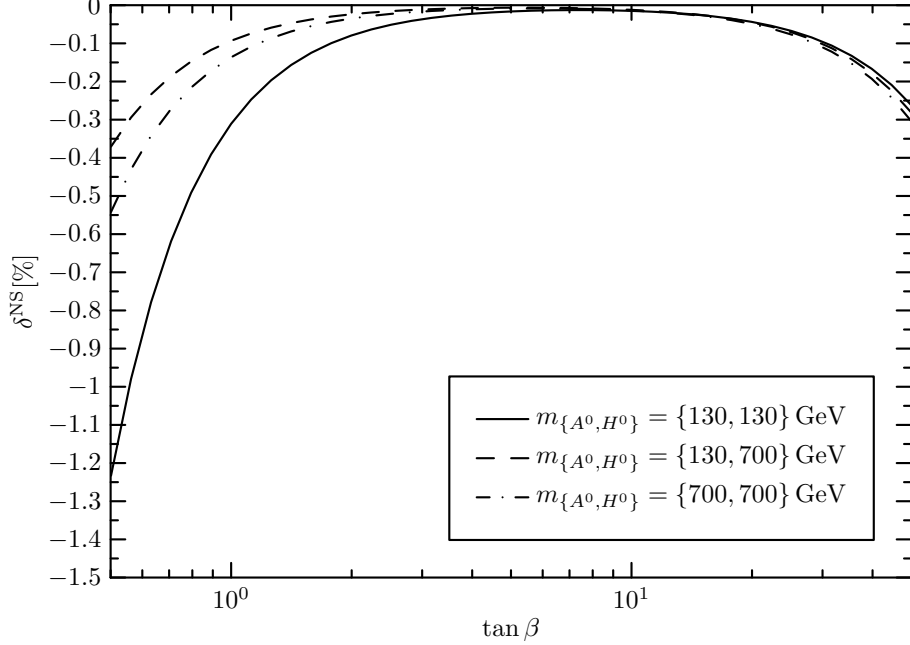


Figure 2: The non-standard correction $\delta_{NS}(G_F)$ to the Born width in the 2HDM as a function of $\tan\beta$ for various Higgs-boson masses. Here $m_{h^0} = 120$ GeV, $m_{H^+} = 320$ GeV, and the angle $\alpha = \beta - \frac{\pi}{2}$.

range which is in accord with experimental constraints:

$$m_{h^0}, m_{H^0}, m_{A^0} \geq 120 \text{ GeV}, \quad m_{H^+} \geq 320 \text{ GeV}, \quad 0.5 \leq \tan\beta \leq 50. \quad (3.2)$$

In Fig. 2 the correction $\delta_{NS}(G_F)$ is shown as a function of $\tan\beta$ for various sets of neutral Higgs masses. Here the mixing angle α was put equal to $\beta - \frac{\pi}{2}$, which means that the couplings of the h^0 become SM-like. For these parameter sets the corrections are negative and become largest in magnitude, of the order of -1% , for $\tan\beta \lesssim 1$, where the Yukawa couplings to the top quark are largest. In Fig. 3 we vary $\tan\beta$ while keeping α fixed and setting $m_{H^0} = 700$ GeV and $m_{A^0} = 130$ GeV. We see that the shape of the curve changes significantly for different values of α . In particular, for $\alpha = 0$, corrections of the order of 0.5% are also possible for intermediate values of $\tan\beta$. However, this strong α dependence disappears if the two scalar Higgs bosons h^0 and H^0 have (approximately) the same mass.

Let us now determine the anomalous form factors $f_{L,R}$ and $g_{L,R}$. They are obtained from the decay amplitude, i.e., the contributions of Fig. 1, by appropriate projections. The form factor f_L is affected by renormalization, while the others are ultraviolet finite.

The bulk of the correction $\delta_{NS}(G_F)$ is due to the renormalized form factor f_L . By scanning the above parameter range we found the following generic features: i) $|f_L| \gg |g_R| \gg |f_R|, |g_L|$ and ii) $|\text{Re} f_L| \gg |\text{Re} g_R| \gg |\text{Im} f_L|, |\text{Im} g_R|$. Hence we display only the real parts of f_L and g_R in the following. Feature i) can be qualitatively understood by inspecting the flow of

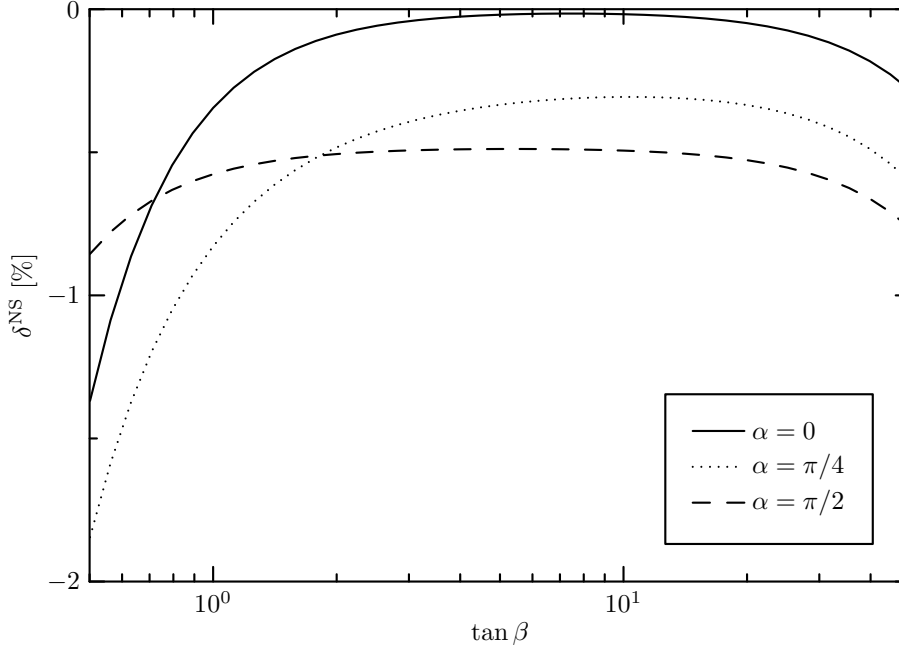


Figure 3: The non-standard correction $\delta_{NS}(G_F)$ to the Born width in the 2HDM as a function of $\tan\beta$ for various (fixed) values of α . Here $m_{h^0} = 120$ GeV, $m_{H^0} = 700$ GeV, $m_{A^0} = 130$ GeV and $m_{H^\pm} = 320$ GeV.

chirality in the diagrams of Fig. 1. As to ii), this follows from the fact that in the parameter range (3.2) only diagrams Fig. 1 (e) and (g) have imaginary parts.

In Fig. 4 the real part of f_L is shown as a function of $\tan\beta$ for the same parameter sets as used in Fig. 2. One sees that $\text{Re } f_L \approx \delta_{NS}/2$, as expected.

Fig. 5 shows the chirality flipping coupling $\text{Re } g_R$ as a function of $\tan\beta$ for the same parameter sets as used in Fig. 4. This anomalous form factor is one order of magnitude smaller than $\text{Re } f_L$ – even for small (large) values of $\tan\beta$ where the Yukawa couplings of the top (bottom) quark become largest. If the mass difference between the two scalar Higgs bosons h^0 and H^0 is large, the form factors depend significantly on the mixing angle α . Fig. 6 shows the $\tan\beta$ dependence of $\text{Re } g_R$ for several fixed values of α and the same parameter sets as the ones used in Fig. 3. Note that varying α can change the sign of $\text{Re } g_R$. The corresponding plot for $\text{Re } f_L$ is not shown, since the relation $|\text{Re } f_L| \gg |\text{Re } g_R|$ holds for all values of α and thus $\text{Re } f_L \approx \delta^{\text{NS}}/2$ for all α .

Neutral Higgs sector CP violation is also possible in 2HDM – already at Born level. (Cf., for instance, the recent discussion in [71].) If the tree-level Higgs potential is not CP -invariant, the states h^0, H^0 can mix with A^0 . Then the 3 neutral physical Higgs-boson mass eigenstates ϕ_i are no longer CP eigenstates; i.e., they couple both to scalar and pseudoscalar quark and lepton currents. The CP eigenstates $\phi' = (h^0, H^0, A^0)$ are related to the mass eigenstates

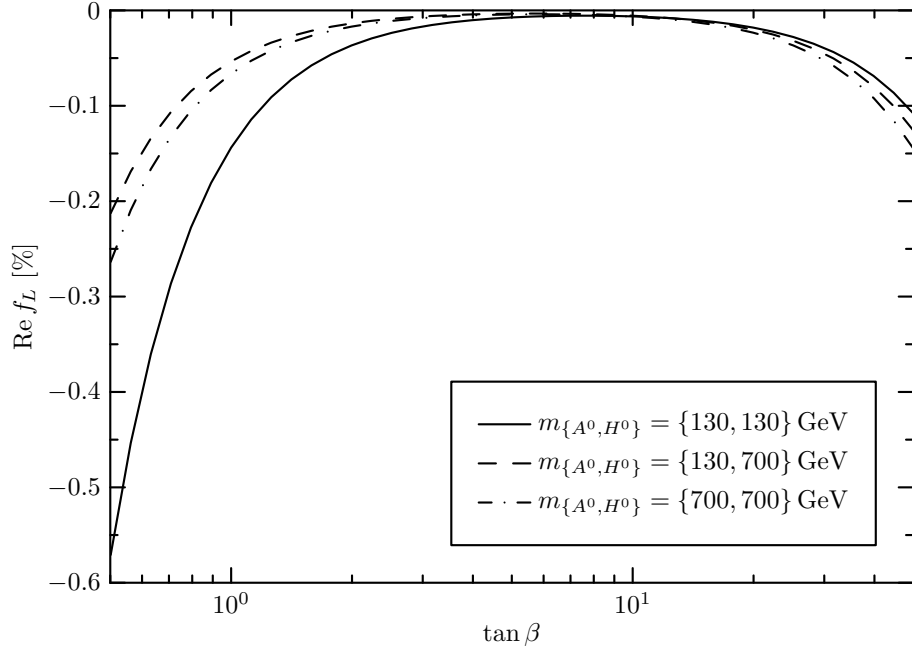


Figure 4: The anomalous form factor $\text{Re } f_L$ in the 2HDM as a function of $\tan\beta$ for various Higgs-boson masses. The remaining parameters are as in Fig. 2.

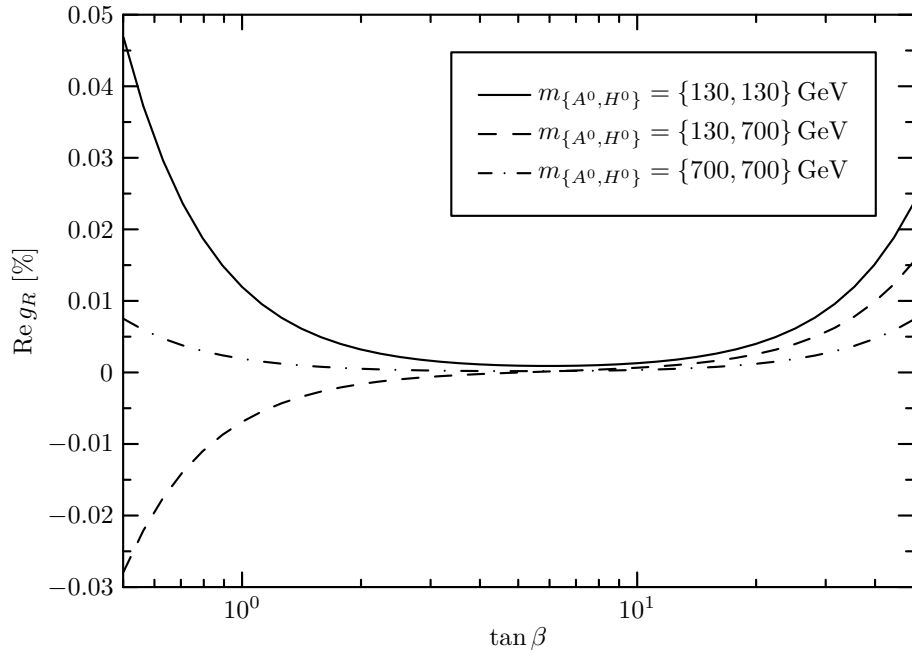


Figure 5: The anomalous form factor $\text{Re } g_R$ in the 2HDM as a function of $\tan\beta$ for various Higgs-boson masses. The remaining parameters are as in Fig. 2.

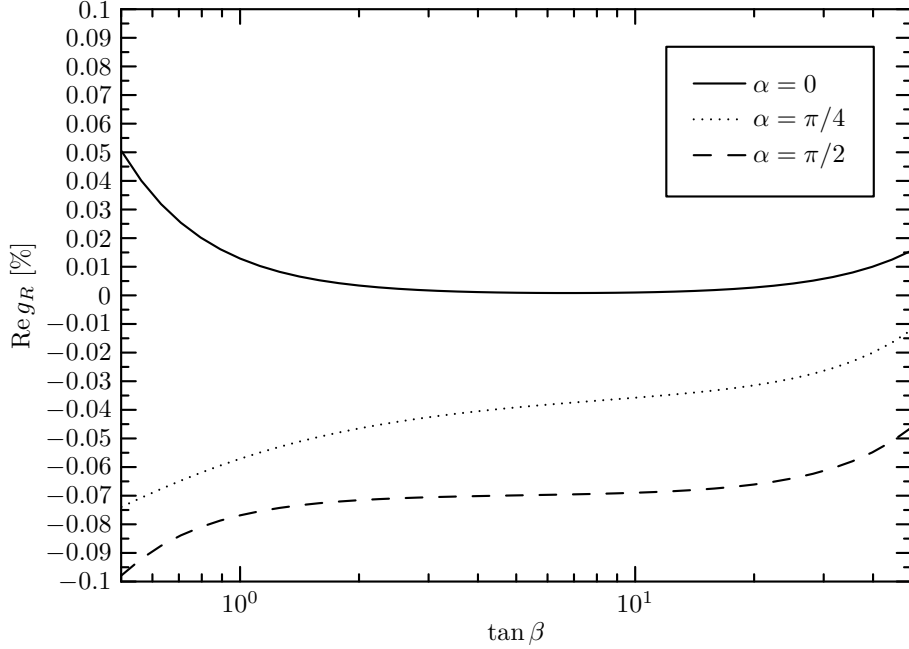


Figure 6: The anomalous form factor $\text{Re } g_R$ in the 2HDM as a function of $\tan\beta$ for various (fixed) values of α . The remaining parameters are as in Fig. 3.

ϕ_i by a real orthogonal matrix R , $\phi'_i = R_{ij}\phi_j$. (See, e.g., [72] for the resulting couplings to fermions and weak gauge bosons). If the neutral Higgs bosons have both scalar and pseudoscalar couplings to the third-generation quarks then, as discussed in Section 2, the form factors acquire imaginary parts – even if the decay amplitude has no absorptive part. With the empirical constraint that $m_{H^+} > m_t$, only the diagrams Fig. 1 (e) and (g) have absorptive parts, of which the piece containing the CP -even (CP -odd) coupling of the ϕ_i to the b quark contributes to the imaginary (real) part of the form factors. We have discarded these imaginary parts in order to determine the size of $\text{Im}f_L$ and $\text{Im}g_R$ due to CP violation. Computing $\text{Im}f_L$ and $\text{Im}g_R$ by scanning the parameter range (3.2) and varying the angles of the mixing matrix R , we find that these couplings do not exceed a few $\times 10^{-4}$. Effects are largest if one of the neutral states ϕ_i is rather light and the other two are heavy and the top-Yukawa couplings of the light Higgs boson are large. Choosing $m_{\phi_1} = 120$ GeV, $m_{\phi_2} = m_{\phi_3} = 700$ GeV, $m_{H^+} = 320$ GeV, $\tan\beta = 1$, and parameterizing the mixing matrix $R = R(\alpha_i)$ in terms of three Euler angles α_i , we have plotted in Fig. 7 the CP -violating contributions to $\text{Im}f_L$ and to $\text{Im}g_R$ as a function of α_2 , for fixed values of α_1 and α_3 . One sees that $|\text{Im}f_L| \leq 5 \times 10^{-4}$ and $|\text{Im}g_R| \leq 3.5 \times 10^{-4}$.

In [51, 73–75] the form factor $\text{Im}g_R$ was analyzed, with which our results are in accord. The couplings $\text{Im}f_L$, $\text{Im}g_R$ are too small to cause observable CP -violating effects, i.e. a decay rate asymmetry (2.9) or a non-zero triple correlation A_- (cf. eq. (2.10)) of the order of 1%

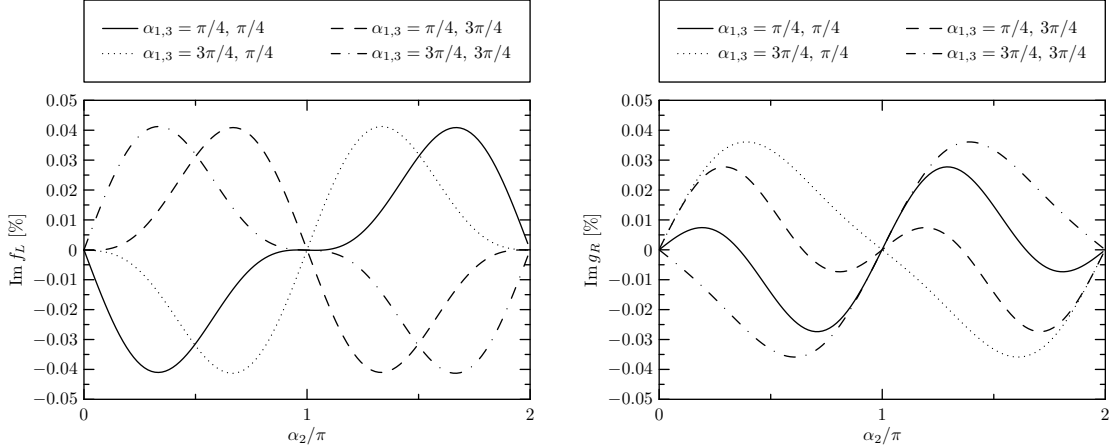


Figure 7: Contributions to $\text{Im } f_L$ (left frame) and to $\text{Im } g_R$ (right frame) from CP -violating neutral Higgs-boson exchange in the 2HDM as a function of the mixing angle α_2 . The remaining parameters are given in the text.

or larger.

3.1.1. The MSSM

Next we analyze the anomalous form factors within the minimal supersymmetric extension of the SM (MSSM). The Higgs sector of the MSSM corresponds to a type-II 2HDM with a CP -invariant tree-level Higgs potential. Thus the Higgs-boson contributions to the $t \rightarrow bW$ decay amplitude are those depicted in Fig. 1. As to the parameters of the MSSM Higgs sector: It is well-known that one of the neutral scalar Higgs bosons, h^0 , is predicted to be light, $m_{h^0} \lesssim 130$ GeV. Moreover, the lower bound on the mass of the charged Higgs boson H^+ from $B(\bar{B} \rightarrow X_s \gamma)$ mentioned above does not apply to the MSSM, as the contribution of H^+ to the amplitude of this decay mode can be compensated to a large extent by the contributions of supersymmetric particles. Thus the mass of H^+ can still be as low as $m_{H^+} \sim 100$ GeV. The experimental lower bound on the mass of the lightest neutral Higgs boson [63] implies that $\tan \beta \gtrsim 3$ in the MSSM.

The “genuine” one-loop MSSM corrections to the $t \rightarrow bW$ decay amplitude are SUSY QCD corrections due to the exchange of gluinos \tilde{g} and squarks $\tilde{q}_{1,2}$, and SUSY electroweak (SUSY EW) corrections which arise from the exchange of squarks, charginos $\tilde{\chi}_i^\pm$, and neutralinos $\tilde{\chi}_i^0$. The corresponding Feynman diagrams are depicted in Fig. 8. We neglect squark-mixing between different generations; i.e., only top and bottom squarks $\tilde{t}_{1,2}$, $\tilde{b}_{1,2}$ are taken into account. These mass eigenstates are mixtures of the respective weak eigenstates.

The SUSY QCD and SUSY EW contributions to the top-width $\Gamma(t \rightarrow bW)$ were computed in [21–23,26] and [24–26], respectively. These contributions tend to cancel each other: while

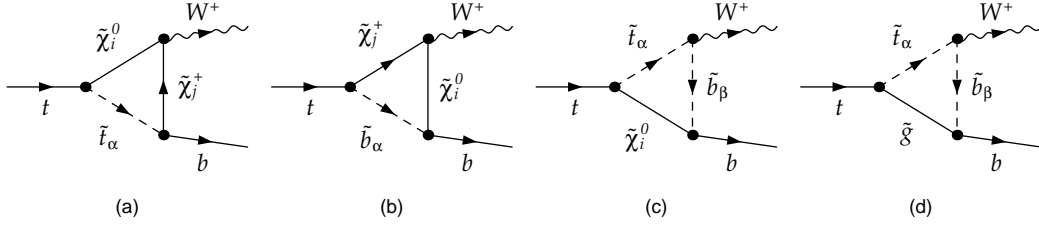


Figure 8: Feynman diagrams for the 1-loop SUSY electroweak (a - c) and QCD (d) contributions to the tbW vertex in the MSSM. The contributions to the two-point functions that are involved in the renormalization are not shown.

the SUSY QCD are in general negative and typically $\lesssim 1\%$ or below in magnitude, the SUSY EW corrections are positive in general and also $\lesssim 1\%$ for phenomenologically acceptable SUSY particle masses. The SUSY QCD and SUSY EW corrections to the helicity fractions $F_{0,\mp}$ defined in Section 2 were calculated in [26]. The corrections to these ratios are typically of the order of 1%, and tend to be of opposite sign. We have also computed these corrections to the top-width. We compared the SUSY QCD corrections with the results of [23, 26], with which we agree.

In the following we assume the masses of the gluinos and of the bottom squarks $\tilde{b}_{1,2}$ to be above 350 GeV, which is suggested by the Tevatron searches and analyses in the context of the mSUGRA scenario (see, e.g., [63]). As to the top squarks $\tilde{t}_{1,2}$, it is not yet excluded that one of them is lighter than the top quark. We assume that $m_{\tilde{t}_1} \geq 100$ GeV. For the masses of the charginos and neutralinos we assume the lower bounds $m_{\tilde{\chi}^+} \geq 100$ GeV, $m_{\tilde{\chi}^0} \geq 50$ GeV.

More specifically, we use the following set of SUSY parameters:

$$\begin{aligned}
\mu &= 250 \text{ GeV}, & M_1 &= 62 \text{ GeV}, & M_2 &= 130 \text{ GeV}, & m_{H^+} &= 250 \text{ GeV}, \\
M_{L_i} &= M_{E_i} = M_{Q_i} = M_{D_i} = M_{U_{1,2}} &= 400 \text{ GeV}, & M_{U_3} &= 250 \text{ GeV}, \\
A_{L_i} &= A_{U_{1,2}} = A_{D_i} = 0, & A_{U_3} &= 700 \text{ GeV}, \\
m_{\tilde{g}} &= 350 \text{ GeV}.
\end{aligned} \tag{3.3}$$

Here μ , M_1 , and M_2 are the soft SUSY breaking masses of the Higgs potential, M_L and M_E are the soft masses of the left and right-handed sleptons, M_Q the soft masses of the left-handed squarks and M_U and M_D the soft masses of the right-handed up- and down-type squarks. We impose the GUT relation $M_1 = 5s_W^2 M_2 / (3c_W^2)$. Furthermore $m_{\tilde{g}}$ is the gluino mass and i is a generation index. Keeping the above parameters fixed and varying $\tan\beta$ between 5 and 50 causes the physical masses and mixing angles to vary in the ranges shown in table 2. The Higgs-boson masses and the mixing angle α in table 2 were calculated with *FeynHiggs* (version 2.6.4) [76–79].

	$\tan\beta = 3$	$\tan\beta = 50$		$\tan\beta = 5$	$\tan\beta = 50$
m_{h_0}	115 GeV	120 GeV	$m_{\tilde{t}_1}$	131 GeV	99 GeV
m_{H_0}	238 GeV	232 GeV	$m_{\tilde{t}_2}$	511 GeV	518 GeV
m_{A_0}	237 GeV	236 GeV	$\theta_{\tilde{t}}$	0.19π	0.19π
α	-0.092π	-0.002π	$m_{\tilde{b}_1}$	395 GeV	319 GeV
$m_{\chi_1^+}$	105 GeV	115 GeV	$m_{\tilde{b}_2}$	409 GeV	471 GeV
$m_{\chi_1^0}$	56 GeV	60 GeV	$\theta_{\tilde{b}}$	-0.23π	-0.25π

Table 2: The values of physical MSSM masses and mixing angles for $\tan\beta = 5$ and $\tan\beta = 50$. Mass eigenvalues are enumerated in ascending order. For example, $m_{\chi_1^0}$ denotes the mass of the lightest neutralino. All other sfermion masses lie at 400 ± 5 GeV for both values of $\tan\beta$. The angles $\theta_{\tilde{t}}$ and $\theta_{\tilde{b}}$ are the stop and sbottom mixing angles, respectively. Since we set all lepton and light (i.e. generation 1 and 2) quark masses to zero, all other mixing angles are zero.

In Fig. 9 the MSSM Higgs, QCD, and EW corrections $\delta_{NS}(G_F) = (\Gamma_{NS} - \Gamma_B(G_F))/\Gamma_B(G_F)$ and their sum are shown as a function of $\tan\beta$. For the parameters specified above, the MSSM Higgs contributions are very small. The SUSY EW contributions have a sharp peak at $\tan\beta \approx 10$, which corresponds to a threshold effect. Here the masses are such that a top quark can decay into an on-shell neutralino and an on-shell stop. Obviously, our results are unreliable in the vicinity of that peak. Otherwise, the MSSM corrections are dominated by the SUSY QCD contributions, which remain almost constant at about -0.6% for $\tan\beta > 10$. In this range, the SUSY EW contributions yield a constant $+0.1\%$, leading to an overall correction of -0.5% .

The bulk of the corrections $\delta_{NS}(G_F)$ is again due to the renormalized form factor f_L . For the parameters given above we found the following features: $|f_L| > |g_R| \gg |f_R|, |g_L|$ and $|\text{Re } f_L|, |\text{Re } g_R| \gg |\text{Im } f_L|, |\text{Im } g_R|$. Therefore we display only $\text{Re } f_L$ and $\text{Re } g_R$.

In Figs. 10 and 11 the real parts of f_L and g_R induced by the various MSSM corrections are shown as a function of $\tan\beta$ for the above parameter set. In the latter case, the Higgs and SUSY EW corrections cancel almost exactly. Thus $\text{Re } g_R$ and $\text{Re } f_L$ are essentially due to the SUSY QCD contribution.

For completeness, we briefly address also the effect of supersymmetric CP -violating phases. As is well known, many new CP phases can be present in the MSSM in general. In order to assess the size of SUSY CP violation it is useful to consider a simplified scenario where, in a certain phase convention, observable CP phases reside only in the μ parameter of the bilinear term in the Higgs superfields and in the trilinear couplings A_f . The experimental upper bounds on the electric dipole moments of the electron, the neutron, and certain atoms

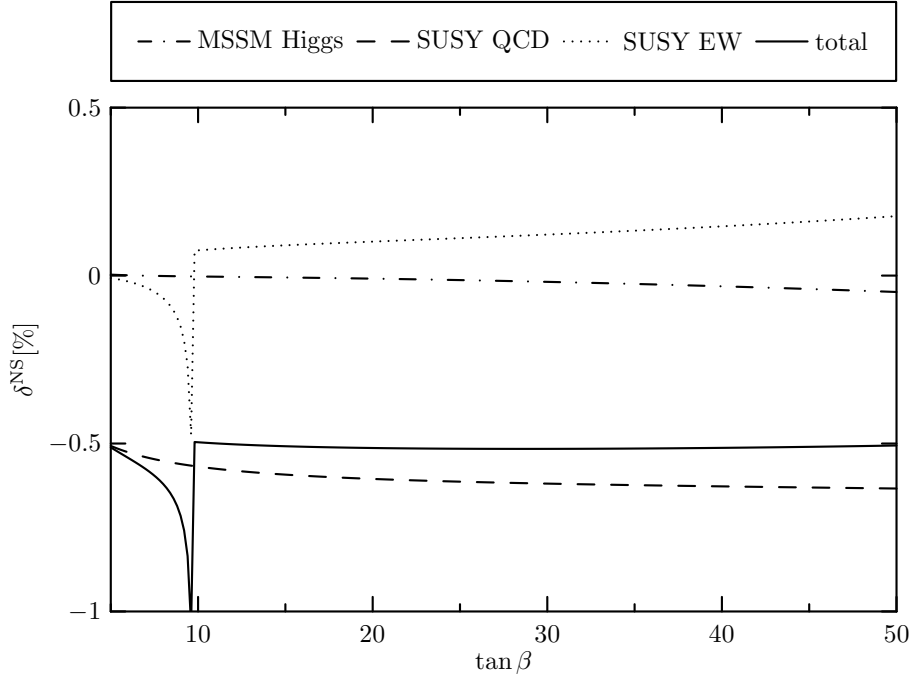


Figure 9: The MSSM Higgs, QCD, and EW corrections $\delta_{NS}(G_F)$ to the Born width as a function of $\tan\beta$. The other parameters are as given in table 2.

constrain the phases of μ and of A_f for the first two generations to very small values (see, for instance, [80]). However, the phases of $A_{t,b}$ may be of order one. This generates CP -violating interactions between gauginos and quarks and squarks of the third generation⁶. Then the imaginary parts of the anomalous form factors receive also contributions induced by the CP phases $\arg(A_{t,b})$, which in turn generate a non-zero triple-correlation asymmetry $\langle O \rangle - \langle \bar{O} \rangle$, discussed in Section 2, or a difference A_{CP} in the partial rates (cf. eq. (2.9)). Such effects were discussed before in [51, 82–84]. For SUSY particle masses used above, these effects are below 0.1%.

⁶In addition, neutral Higgs sector CP violation is induced at the 1-loop level, which may be sizeable [81].

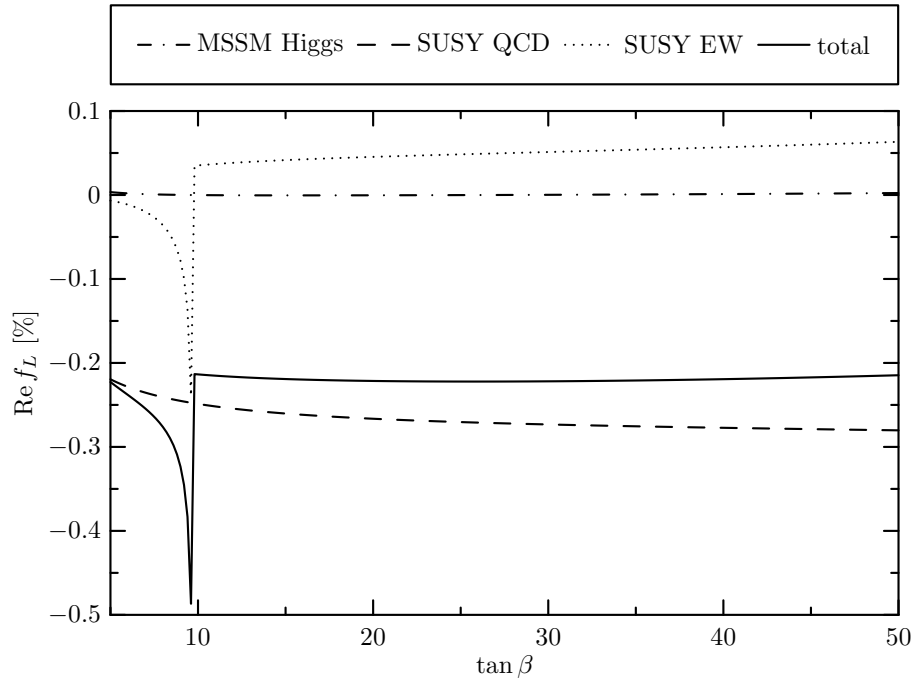


Figure 10: The anomalous form factor $\text{Re } f_L$ induced by the MSSM Higgs, QCD, and EW corrections as a function of $\tan\beta$. The other parameters are as given in table 2.

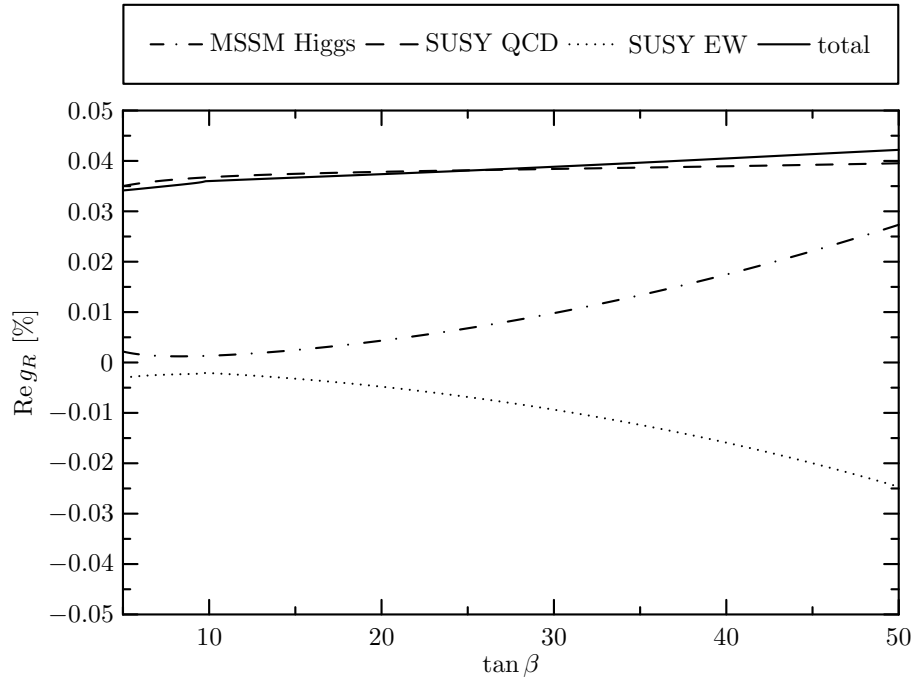


Figure 11: The anomalous form factor $\text{Re } g_R$ induced by the MSSM Higgs, QCD, and EW corrections as a function of $\tan\beta$. The other parameters are as given in table 2.

3.1.2. Top-color assisted technicolor and Little Higgs models

The concept that electroweak symmetry breaking (EWSB) and the generation of quark and lepton masses occur “dynamically” by the condensation of (new) fermion-antifermion pairs is still an alternative to the Higgs mechanism not ruled out by experiment. Among the phenomenologically acceptable models that use this concept is top-color assisted technicolor (TC2) [85, 86]. TC2 has two strongly interacting sectors in order to explain EWSB and the large top-quark mass. Technicolor interactions (TC) are responsible, via the condensation of techni-fermions, $\langle \bar{T}T \rangle$ ($T = U, D$), for most of EWSB, but they contribute very little to the top-quark mass m_t , while top-color interactions (TopC) generate through condensation of top quarks, $\langle \bar{t}t \rangle$, the bulk of m_t but make only a small contribution to EWSB. The spin-zero states of the model are bound-states of the techni-fermions and of t, b . These two sets of bound-states form two $SU(2)_L$ doublets Φ_{TC}, Φ_t , whose couplings to the weak gauge bosons and to t and b are formally equivalent to a two-Higgs doublet model. The physical spin-zero states are i) a heavy neutral scalar H_{TC} with a mass of order 1 TeV, ii) a neutral scalar H_t which is a $\bar{t}t$ bound state whose mass is expected to be of the order $m_{H_t} \sim 2m_t$ when estimated à la Nambu-Jona-Lasinio, but could also be considerably lighter [87], and iii) a neutral “top-pion” Π^0 and a pair of charged ones, Π^\pm , whose masses are predicted to lie in the range of 180 - 250 GeV [85, 86]. Below we shall use $m_{H_t} \geq 120$ GeV, $m_{\Pi^0} = m_{\Pi^\pm} \geq 180$ GeV, and $m_{H_{TC}} = 1$ TeV.

The Yukawa couplings of the top quark to the physical spin-zero states read after EWSB [88]:

$$\begin{aligned} \mathcal{L}_Y = & -\frac{1}{\sqrt{2}}(Y_t f_\pi + \varepsilon_t v_T) \bar{t}t - \frac{1}{\sqrt{2}}(Y_t H_t + \varepsilon_t H_{TC}) \bar{t}t \\ & - (i \frac{Y_\pi}{\sqrt{2}} \Pi^0 \bar{t}_{LR} + i Y_\pi \Pi^\pm \bar{b}_{LR} + \text{h.c.}), \end{aligned} \quad (3.4)$$

where $Y_\pi = (Y_t v_T - \varepsilon_t f_\pi)/v$. Here f_π denotes the value of the top-quark condensate which is estimated in the TC2 model to be $f_\pi \sim 60$ GeV [85, 88]. Once f_π is fixed, v_T is determined by the EWSB requirement that $f_\pi^2 + v_T^2 = v^2 = (246 \text{ GeV})^2$. From (3.4) one sees that $(Y_t f_\pi + \varepsilon_t v_T)/\sqrt{2} = m_t$. The technicolor contribution ε_t to the top mass is small, by construction of the TC2 model. We have therefore set $\varepsilon_t = 0$ in our calculation. As a consequence the top Yukawa coupling Y_t becomes large, i.e. $Y_t \simeq 4$. Therefore, the top quark is expected to couple strongly to H_t and to the top-pions. The coupling of the charged top-pion to b_R is very small, and likewise the couplings of Π^0 and H_t to b quarks. We shall therefore neglect them below. The remaining interactions of the two doublets Φ_{TC}, Φ_t with t, b and with the weak gauge bosons can be found in [88] whose conventions we use here.

The 1-loop new physics contributions in the TC2 model to the $t \rightarrow bW$ decay amplitude correspond to the diagrams of Fig. 1 with the replacements $h^0 \rightarrow H_{TC}$, $H^0 \rightarrow H_t$, $A^0 \rightarrow \Pi^0$, and $H^\pm \rightarrow \Pi^\pm$. In addition there are the 1-loop contributions of these spin-zero states

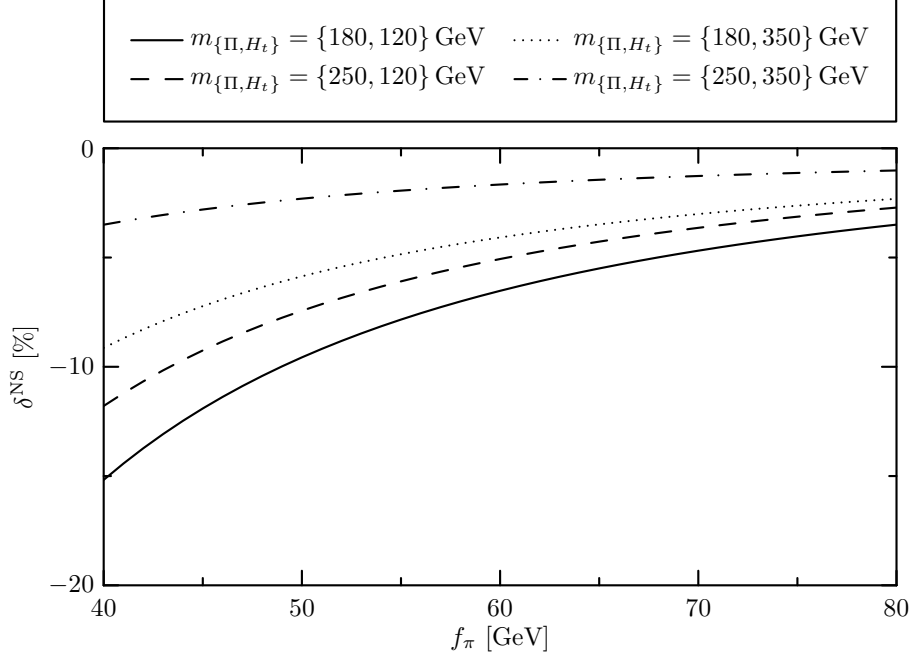


Figure 12: The correction $\delta_{NS}(G_F)$ to the Born width in the TC2 model as a function of f_π .

to the wave-function renormalization constants and to Δr . As H_{TC} is very heavy and its Yukawa couplings to t and b are small, the contributions of the corresponding diagrams are suppressed with respect to the remaining corrections. The same remark applies to the diagrams where Π^0 and H_t couple to b quarks. A closer inspection shows that, for relatively light $\Pi^{0,\pm}$ and H_t the two dominant contributions are Fig. 1 (b) with $\phi_i = H_t$ and $\phi_i = \Pi^0$ while Figs. 1(d) and (f) are subdominant.

The corrections to the top-width and to the helicity fractions were computed in [27], in the conventional on-shell renormalization scheme (α_{em} scheme, for a TC2 model slightly different from that outlined in [88]). Using the couplings and masses of [27] we find agreement with this this paper.

Fig. 12 shows the correction $\delta_{NS}(G_F) = (\Gamma_{NS} - \Gamma_B(G_F))/\Gamma_B(G_F)$ as a function of the value of the top-quark condensate f_π , for various sets of masses m_{H_t} , m_Π of the top-Higgs boson and top-pions. For fixed m_{H_t} , m_Π the corrections increase in magnitude with increasing top-Yukawa coupling, i.e., decreasing f_π . As mentioned above, the dominant contributions are the ones corresponding to Fig. 1 (b) with $\phi_i = H_t$ and $\phi_i = \Pi^0$. The correction $\delta_{NS}(G_F)$ is negative in the above parameter range. It can become as large as $\sim -15\%$.

The renormalized form factor $\text{Re } f_L$ is plotted in Fig. 13 as a function of f_π . As expected, $\text{Re } f_L \approx \delta_{NS}/2$. The chirality-flipping form factor $\text{Re } g_R$ is shown in Fig. 14. The magnitude of this form factor remains below the percent level also in this model.

For completeness, we mention some results from Little Higgs models. These models in-

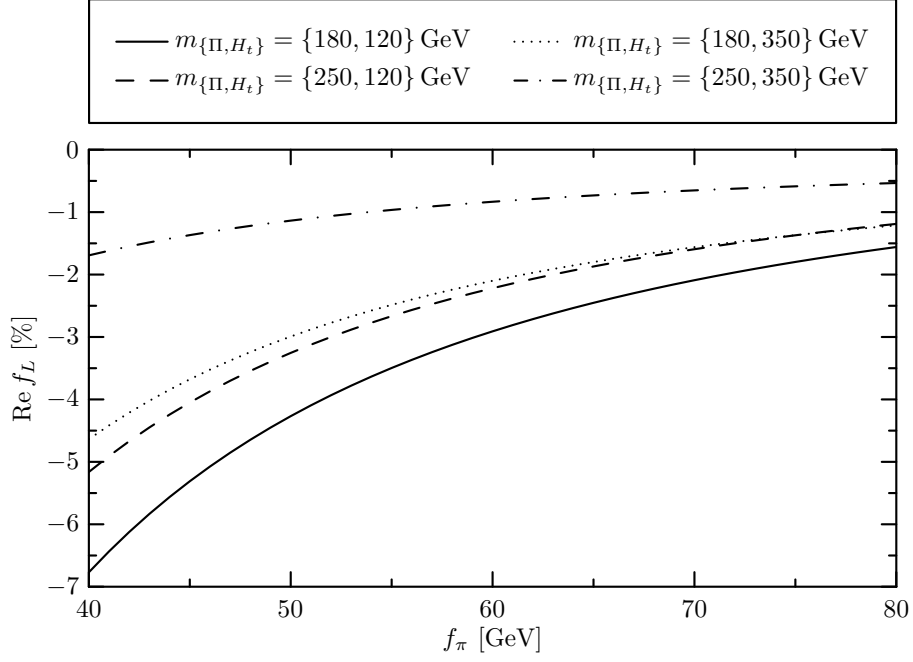


Figure 13: The anomalous form factor $\text{Re } f_L$ in the TC2 model as a function of f_π .

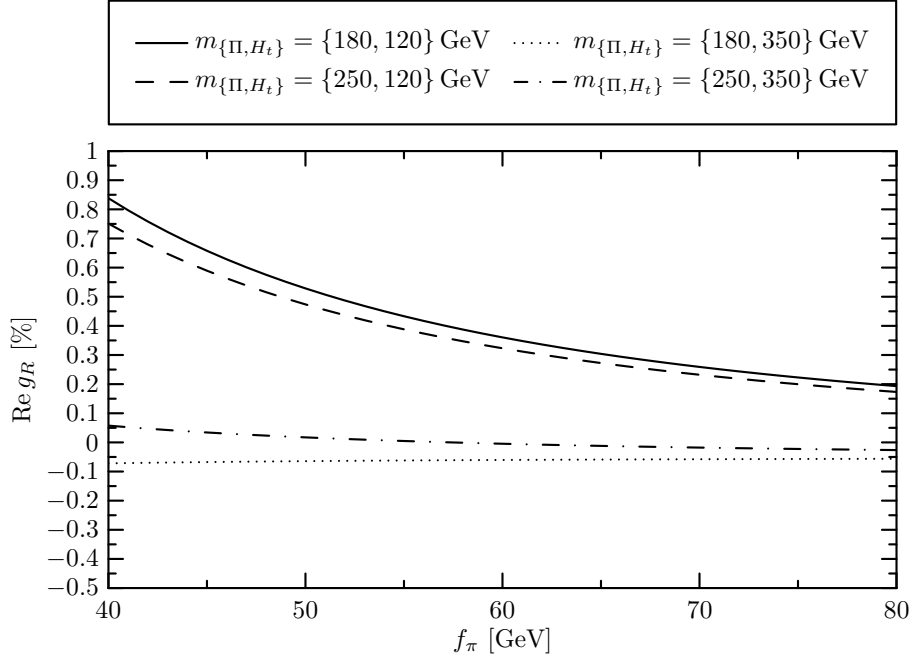


Figure 14: The anomalous form factor $\text{Re } g_R$ in the TC2 model as a function of f_π .

corporate heavy partners (with TeV scale masses) of the weak gauge bosons and of the top quark. An often studied version of these models is the “Littlest Higgs” model (LH) [89] with T -parity symmetry [90]. In this model, the SM tbW vertex is modified already at tree-level due to the mixing of t_L with the heavy top-quark partner T and the mixing of the weak gauge bosons W^\pm with their heavy partners W_H^\pm . The resulting anomalous coupling f_L and the correction to the top-quark decay width $\delta\Gamma_t/\Gamma_t$ are negative; the latter can become larger than 10% in magnitude [28, 29]. One-loop LH radiative corrections induce also a coupling $\text{Re}g_R$ which is, however, too small to be observable at the LHC [30].

4. Conclusions

In this paper we have analyzed the magnitudes and phases of the anomalous form factors $f_{L,R}$ and $g_{L,R}$ in the tWb vertex within several SM extensions, to wit, a 2HDM, the MSSM, and a TC2 model. We found that the imaginary parts of the form factors, which can be induced either by CP -invariant final-state rescattering or by CP -violating interactions, are very small compared to the real parts. Moreover, within the above models, $|\text{Re}f_R|, |\text{Re}g_L| \ll |\text{Re}g_R| < |\text{Re}f_L|$. In the 2HDM and the MSSM, where electroweak symmetry breaking is triggered by elementary Higgs fields, the magnitudes of the anomalous couplings f_L, g_R are smaller than 1%. TC2 and Little Higgs models are viable paradigms for the special role the top can play in the mechanism of electroweak symmetry breaking. TC2 interactions may reduce f_L significantly, which would reduce the top width by 10% or more. A reduction of similar size can happen in Little Higgs models. In the long run, this can be tested in single-top-quark production at the LHC, where one may eventually measure f_L with a precision of about 5%. The determination of the top width Γ_t with an accuracy of about 10% would require a high-energy e^+e^- linear collider [91], where Γ_t could be obtained from a precision measurement of $t\bar{t}$ production at threshold.

Acknowledgments

We wish to thank Peter Zerwas for useful discussions and J. j. Cao for a correspondence concerning Ref. [26]. This work was supported by Deutsche Forschungsgemeinschaft SFB/TR9.

References

- [1] E. W. Varnes [CDF and D0 Collaborations], arXiv:0810.3652 [hep-ex].
- [2] D. Chakraborty, J. Konigsberg and D. L. Rainwater, Ann. Rev. Nucl. Part. Sci. **53** (2003) 301 [arXiv:hep-ph/0303092].
- [3] W. Wagner, Rept. Prog. Phys. **68** (2005) 2409 [arXiv:hep-ph/0507207].
- [4] A. Quadt, Eur. Phys. J. C **48** (2006) 835.
- [5] W. Bernreuther, J. Phys. G **35** (2008) 083001 [arXiv:0805.1333 [hep-ph]].
- [6] A. Abulencia *et al.* [CDF II Collaboration], Phys. Rev. D **75** (2007) 052001 [arXiv:hep-ex/0612011].
- [7] A. Abulencia *et al.* [CDF Collaboration], Phys. Rev. Lett. **98** (2007) 072001 [arXiv:hep-ex/0608062].
- [8] V. M. Abazov *et al.* [D0 Collaboration], Phys. Rev. D **75** (2007) 031102 [arXiv:hep-ex/0609045].
- [9] V. M. Abazov *et al.* [D0 Collaboration], Phys. Rev. Lett. **100** (2008) 062004 [arXiv:0711.0032 [hep-ex]].
- [10] V. M. Abazov *et al.* [D0 Collaboration], Phys. Rev. Lett. **98** (2007) 181802 [arXiv:hep-ex/0612052].
- [11] V. M. Abazov *et al.* [D0 Collaboration], Phys. Rev. D **78**, 012005 (2008) [arXiv:0803.0739 [hep-ex]].
- [12] V. M. Abazov *et al.* [D0 Collaboration], arXiv:0807.1692 [hep-ex].
- [13] T. Aaltonen *et al.* [CDF Collaboration], arXiv:0809.2581 [hep-ex].
- [14] F. Hubaut, E. Monnier, P. Pralavorio, K. Smolek and V. Simak, Eur. Phys. J. C **44** **S2** (2005) 13 [arXiv:hep-ex/0508061].
- [15] S. Tsuno, I. Nakano, Y. Sumino and R. Tanaka, Phys. Rev. D **73** (2006) 054011 [arXiv:hep-ex/0512037].
- [16] J. A. Aguilar-Saavedra, J. Carvalho, N. Castro, F. Veloso and A. Onofre, Eur. Phys. J. C **50** (2007) 519 [arXiv:hep-ph/0605190].

- [17] J. A. Aguilar-Saavedra, J. Carvalho, N. Castro, A. Onofre and F. Veloso, Eur. Phys. J. C **53** (2008) 689 [arXiv:0705.3041 [hep-ph]].
- [18] J. A. Aguilar-Saavedra, Nucl. Phys. B **804** (2008) 160 [arXiv:0803.3810 [hep-ph]].
- [19] B. Grzadkowski and W. Hollik, Nucl. Phys. B **384** (1992) 101.
- [20] A. Denner and A. H. Hoang, Nucl. Phys. B **397** (1993) 483.
- [21] C. S. Li, J. M. Yang and B. Q. Hu, Phys. Rev. D **48** (1993) 5425.
- [22] A. Dabelstein, W. Hollik, C. Jünger, R. A. Jimenez and J. Sola, Nucl. Phys. B **454** (1995) 75 [arXiv:hep-ph/9503398].
- [23] A. Brandenburg and M. Maniatis, Phys. Lett. B **545** (2002) 139 [arXiv:hep-ph/0207154].
- [24] J. M. Yang and C. S. Li, Phys. Lett. B **320** (1994) 117.
- [25] D. Garcia, R. A. Jimenez, J. Sola and W. Hollik, Nucl. Phys. B **427** (1994) 53 [arXiv:hep-ph/9402341].
- [26] J. j. Cao, R. J. Oakes, F. Wang and J. M. Yang, Phys. Rev. D **68** (2003) 054019 [arXiv:hep-ph/0306278].
- [27] X. l. Wang, Q. l. Zhang and Q. p. Qiao, Phys. Rev. D **71** (2005) 014035 [arXiv:hep-ph/0501145].
- [28] Q. H. Cao, C. S. Li and C. P. Yuan, Phys. Lett. B **668** (2008) 24 [arXiv:hep-ph/0612243].
- [29] C. F. Berger, M. Perelstein and F. Petriello, arXiv:hep-ph/0512053.
- [30] F. Penunuri and F. Larios, arXiv:0810.4545 [hep-ph].
- [31] J. Alwall *et al.*, Eur. Phys. J. C **49** (2007) 791 [arXiv:hep-ph/0607115].
- [32] W. Bernreuther, O. Nachtmann, P. Overmann and T. Schröder, Nucl. Phys. B **388** (1992) 53 [Erratum-ibid. B **406** (1993) 516].
- [33] M. Jezabek and J. H. Kühn, Phys. Lett. B **329** (1994) 317 [arXiv:hep-ph/9403366].
- [34] W. Bernreuther, M. Fuecker and Y. Umeda, Phys. Lett. B **582** (2004) 32 [arXiv:hep-ph/0308296].
- [35] K. Fujikawa and A. Yamada, Phys. Rev. D **49** (1994) 5890.

- [36] P. L. Cho and M. Misiak, *Phys. Rev. D* **49** (1994) 5894 [arXiv:hep-ph/9310332].
- [37] B. Grzadkowski and M. Misiak, arXiv:0802.1413 [hep-ph].
- [38] F. Larios, M. A. Perez and C. P. Yuan, *Phys. Lett. B* **457** (1999) 334 [arXiv:hep-ph/9903394].
- [39] G. Burdman, M. C. Gonzalez-Garcia and S. F. Novaes, *Phys. Rev. D* **61** (2000) 114016 [arXiv:hep-ph/9906329].
- [40] H. S. Do, S. Groote, J. G. Körner and M. C. Mauser, *Phys. Rev. D* **67** (2003) 091501 [arXiv:hep-ph/0209185].
- [41] C. R. Chen, F. Larios and C. P. Yuan, *Phys. Lett. B* **631** (2005) 126 [AIP Conf. Proc. **792** (2005) 591] [arXiv:hep-ph/0503040].
- [42] E. Boos, L. Dudko and T. Ohl, *Eur. Phys. J. C* **11** (1999) 473 [arXiv:hep-ph/9903215].
- [43] Q. H. Cao, J. Wudka and C. P. Yuan, *Phys. Lett. B* **658** (2007) 50 [arXiv:0704.2809 [hep-ph]].
- [44] M. M. Najafabadi, *JHEP* **0803** (2008) 024 [arXiv:0801.1939 [hep-ph]].
- [45] C. A. Nelson, B. T. Kress, M. Lopes and T. P. McCauley, *Phys. Rev. D* **56** (1997) 5928 [arXiv:hep-ph/9707211].
- [46] C. A. Nelson and A. M. Cohen, *Eur. Phys. J. C* **8** (1999) 393 [arXiv:hep-ph/9806373].
- [47] C. A. Nelson and L. J. . Adler, *Eur. Phys. J. C* **17** (2000) 399 [arXiv:hep-ph/0007086].
- [48] J. P. Lee and K. Y. Lee, arXiv:0806.1389 [hep-ph].
- [49] J. P. Ma and A. Brandenburg, *Z. Phys. C* **56** (1992) 97.
- [50] K. Hagiwara, K. Mawatari and H. Yokoya, *JHEP* **0712** (2007) 041 [arXiv:0707.3194 [hep-ph]].
- [51] W. Bernreuther and P. Overmann, *Z. Phys. C* **61** (1994) 599.
- [52] G. Mahlon and S. J. Parke, *Phys. Lett. B* **476** (2000) 323 [arXiv:hep-ph/9912458].
- [53] M. Jezabek and J. H. Kühn, *Nucl. Phys. B* **314** (1989) 1.
- [54] A. Denner and T. Sack, *Nucl. Phys. B* **358** (1991) 46.
- [55] G. Eilam, R. R. Mendel, R. Migneron and A. Soni, *Phys. Rev. Lett.* **66** (1991) 3105.

- [56] A. Czarnecki and K. Melnikov, Nucl. Phys. B **544** (1999) 520 [arXiv:hep-ph/9806244].
- [57] K. G. Chetyrkin, R. Harlander, T. Seidensticker and M. Steinhauser, Phys. Rev. D **60** (1999) 114015 [arXiv:hep-ph/9906273].
- [58] M. Jezabek and J. H. Kühn, Nucl. Phys. B **320** (1989) 20.
- [59] A. Czarnecki, M. Jezabek and J. H. Kühn, Nucl. Phys. B **351** (1991) 70.
- [60] M. Fischer, S. Groote, J. G. Körner and M. C. Mauser, Phys. Rev. D **65** (2002) 054036 [arXiv:hep-ph/0101322].
- [61] A. Brandenburg, Z. G. Si and P. Uwer, Phys. Lett. B **539** (2002) 235 [arXiv:hep-ph/0205023].
- [62] G. Abbiendi *et al.* [OPAL Collaboration], Eur. Phys. J. C **40** (2005) 317 [arXiv:hep-ex/0408097].
- [63] C. Amsler *et al.* [Particle Data Group], Phys. Lett. B **667** (2008) 1.
- [64] P. Gambino and M. Misiak, Nucl. Phys. B **611** (2001) 338 [arXiv:hep-ph/0104034].
- [65] T. Hahn, Comput. Phys. Commun. **140**, 418 (2001) [arXiv:hep-ph/0012260].
- [66] T. Hahn and C. Schappacher, Comput. Phys. Commun. **143**, 54 (2002) [arXiv:hep-ph/0105349].
- [67] T. Hahn and M. Perez-Victoria, Comput. Phys. Commun. **118**, 153 (1999) [arXiv:hep-ph/9807565].
- [68] T. Hahn, Nucl. Phys. Proc. Suppl. **116**, 363 (2003) [arXiv:hep-ph/0210220].
- [69] T. Hahn, Nucl. Phys. Proc. Suppl. **135**, 333 (2004) [arXiv:hep-ph/0406288].
- [70] T. Hahn and M. Rauch, Nucl. Phys. Proc. Suppl. **157**, 236 (2006) [arXiv:hep-ph/0601248].
- [71] M. Maniatis, A. von Manteuffel and O. Nachtmann, arXiv:0707.3344 [hep-ph].
- [72] W. Bernreuther, T. Schröder and T. N. Pham, Phys. Lett. B **279** (1992) 389.
- [73] B. Grzadkowski and J. F. Gunion, Phys. Lett. B **287** (1992) 237.
- [74] T. Hasuike, T. Hattori, T. Hayashi and S. Wakaizumi, Z. Phys. C **76** (1997) 127 [arXiv:hep-ph/9611304].

- [75] T. Hasuike, T. Hattori and S. Wakaizumi, Phys. Rev. D **58** (1998) 095008 [arXiv:hep-ph/9911526].
- [76] S. Heinemeyer, W. Hollik and G. Weiglein, Comput. Phys. Commun. **124** (2000) 76 [arXiv:hep-ph/9812320].
- [77] S. Heinemeyer, W. Hollik and G. Weiglein, Eur. Phys. J. C **9**, 343 (1999) [arXiv:hep-ph/9812472].
- [78] G. Degrassi, S. Heinemeyer, W. Hollik, P. Slavich and G. Weiglein, Eur. Phys. J. C **28**, 133 (2003) [arXiv:hep-ph/0212020].
- [79] M. Frank, T. Hahn, S. Heinemeyer, W. Hollik, H. Rzehak and G. Weiglein, JHEP **0702**, 047 (2007) [arXiv:hep-ph/0611326].
- [80] M. Pospelov and A. Ritz, Annals Phys. **318** (2005) 119 [arXiv:hep-ph/0504231].
- [81] A. Pilaftsis, Phys. Lett. B **435** (1998) 88 [arXiv:hep-ph/9805373].
- [82] B. Grzadkowski and W. Y. Keung, Phys. Lett. B **319** (1993) 526 [arXiv:hep-ph/9310286].
- [83] E. Christova and M. Fabbrichesi, Phys. Lett. B **320** (1994) 299 [arXiv:hep-ph/9307298].
- [84] M. Aoki and N. Oshimo, Nucl. Phys. B **531** (1998) 49 [arXiv:hep-ph/9801294].
- [85] C. T. Hill, Phys. Lett. B **345** (1995) 483 [arXiv:hep-ph/9411426].
- [86] G. Buchalla, G. Burdman, C. T. Hill and D. Komiris, Phys. Rev. D **53** (1996) 5185 [arXiv:hep-ph/9510376].
- [87] R. S. Chivukula, B. A. Dobrescu, H. Georgi and C. T. Hill, Phys. Rev. D **59** (1999) 075003 [arXiv:hep-ph/9809470].
- [88] A. K. Leibovich and D. L. Rainwater, Phys. Rev. D **65** (2002) 055012 [arXiv:hep-ph/0110218].
- [89] N. Arkani-Hamed, A. G. Cohen, E. Katz and A. E. Nelson, JHEP **0207** (2002) 034 [arXiv:hep-ph/0206021].
- [90] H. C. Cheng and I. Low, JHEP **0309** (2003) 051 [arXiv:hep-ph/0308199].
- [91] J. A. Aguilar-Saavedra *et al.* [ECFA/DESY LC Physics Working Group], arXiv:hep-ph/0106315.

